

---

# A Hybrid Meshing Scheme Based on Terrain Feature Identification

Volker Berkhahn<sup>1</sup>, Kai Kaapke<sup>2</sup>, Sebastian Rath<sup>3</sup> and Erik Pasche<sup>3</sup>

<sup>1</sup> University of Hannover, Institute of Computer Science in Civil Engineering, Callinstr. 34, 30167 Hannover, Germany, [berkhahn@bauinf.uni-hannover.de](mailto:berkhahn@bauinf.uni-hannover.de)

<sup>2</sup> University of New South Wales, Water Research Laboratory, King Street, Sydney, 2093, Australia, [k.kaapke@wrl.unsw.edu.au](mailto:k.kaapke@wrl.unsw.edu.au)

<sup>3</sup> University of Technology Hamburg, Department of River and Coastal Engineering, Denickestraße 22, 21073 Hamburg, Germany, [S.Rath@tuhh.de](mailto:S.Rath@tuhh.de), [Pasche@tuhh.de](mailto:Pasche@tuhh.de)

## 1 Abstract

Hydrodynamic engineering makes profitably use of numerical simulations which rely on discrete element meshes of the topography. To cope with specific circumstances in river hydraulics, the presented hybrid meshing scheme comprises following proposals: river beds and areas of significant terrain slopes are meshed with regular elements to support user specified edge ratio and element orientation representing flow gradients appropriately; floodplains are represented as irregular triangle meshes, concatenating disconnected regular meshes while warranting high approximation quality. Automatic breakline detection approximates flow relevant changes in topographic gradients and defines borders of different mesh types. This paper presents an enhanced strategy for a terrain feature analysis based on b-spline analysis grids and on an interpolation scheme for breakline points in order to reduce the zigzag property of detected breaklines. This scheme for terrain analysis and meshing functionality is implemented in the open source software tool HybridMesh.

*Keywords:* Terrain feature analysis, breakline identification, hybrid element meshing scheme, regular meshes on b-spline surfaces, irregular triangle meshes, hydrodynamic simulations based on finite elements.

## 2 Introduction

Hydrodynamic engineering using remote sensing data sources faces growing data volumes for analysis, forecasts and assessments. Numerical simulations of water levels, flow velocities or sediment transport in river and coastal engineering require element meshes approximating the considered topography sufficiently accurate and while representing all significant terrain features. With respect to implementation

and application of these methods, element meshes are supposed to fulfill requirements regarding edge ratio, element angles and element size. In practice, these requirements also vary for different characteristic areas of a flooded domain.

The purpose of the suggested hybrid mesh generation algorithm is to generate meshes for hydrodynamic studies, providing enhanced suitability for numerical simulations schemes. The numerical scheme under consideration describes flow characteristics based on the depth and time averaged Navier-Stokes equations, widely known as shallow water wave equations. The hydrodynamic model for the presented study is an ancestor of the hydrodynamic model RMA2, which is enhanced for roughness and turbulence modeling. RMA2 uses the fully implicit implementation of the Galerkin weighted residual technique, originally developed for the Resource Management Associates in Lafayette. Today, RMA2 is internationally accepted as hydraulic model for two-dimensional steady and unsteady flow and well-suited for mapping inundation areas [FEMA-2004a]. It generally supports the use of triangular and quadrilateral meshes as well as mixed discretisations of the terrain.

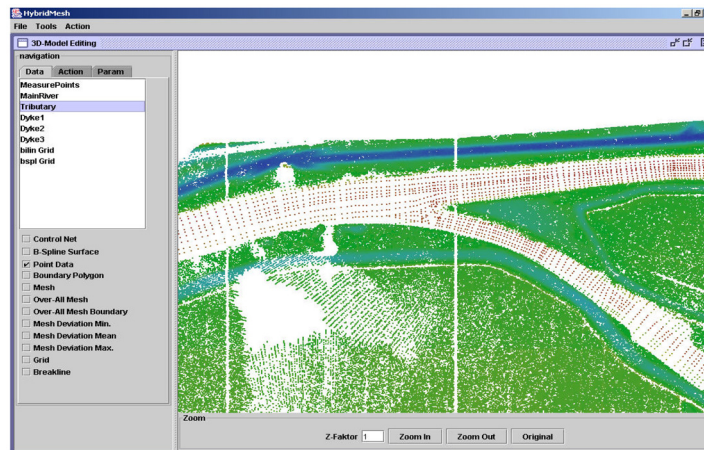


**Fig. 1.** Topography of the River Stoer and the tributary Bramau (case study 1) visualized with the analysis and meshing tool HybridMesh

In this contribution the hybrid meshing scheme is exemplarily demonstrated for two different case studies. Case study 1 represents an alluvial, partly straightened stream: The River Stoer, located in the lowlands in Northern Germany, is a tributary of the River Elbe. The data basis for simulations of this stream are airborne LiDAR topographic survey data in conjunction with bathymetry measurements. Provided as irregular point cloud with variable density, the average resolution of the LiDAR data set offers several measures per square metre. The bathymetry is gathered from profile measurements, compacted via linear interpolation schemes to obtain approximately a 5 m resolution. Fig. 1 shows a plan view on the data set, revealing some lacks in the terrain coverage due to inundation and impact of tiling.

Case study 2 represents a digital terrain model of a tributary to the River Danube. Different characteristics of this topography are obvious: The resolution

of measurement points in the area of the river bed and the river slope is 4 m. In contrast to this, the resolution in the floodplain area is 20 m. In addition to these two different resolution areas, a fine resolution of 1 m is used to describe significant terrain features in the area of the river bed and the floodplain. These different resolution areas of the topography point out the necessity for separate considerations of different meshing areas and for a hybrid meshing scheme. Fig. 2 shows the original data set of case study 2 as well as the identified breaklines marked in red.

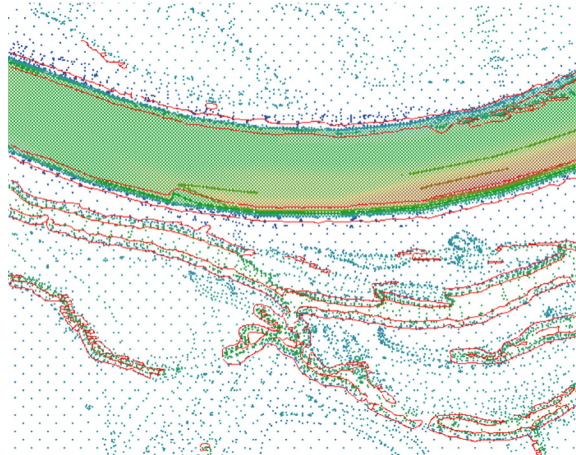


**Fig. 2.** Data set of a tributary to the River Danube with identified breaklines (case study 2)

The software tool HybridMesh combines the functionality of breakline identification [RathPasche-2004] and entirely automated meshing. The irregular triangle meshes are based on a Delaunay refinement [RathBajat-2004] and the regular mesh generation is based on free form surfaces [BerkhahnEtAl-2002], [BerkhahnMai-2004a] [BerkhahnMai-2004b]. This HybridMesh tool is developed by the authors of this paper and is an enhancement of the HydroMesh tool [Goebel-2005]. HybridMesh is implemented with the Java programming language and will be available as open source software.

### 3 Hybrid Meshing Scheme

The hybrid mesh generation scheme presented by Rath et al. [RathEtAl-2005] considers the topography of river beds and their adjacent floodplains individually. A separate consideration of river beds and their floodplains for mesh generation denotes the distinct measurement technologies for these sub domains, their accuracy demands and domination for numeric simulations. The individual consideration of different topographic sub domains is realized based on terrain feature recognition for breakline identification.

### 3.1 Status Quo of the Hybrid Meshing Scheme

The objective of the hybrid meshing scheme is to combine the advantages of regular mesh generation based on b-spline surfaces and irregular triangle meshes generated by a Delaunay refinement.

B-spline surfaces are beneficial for discarding blunders, while providing a topography approximation using regular element meshes, being efficiently with respect to specified edge ratio and element orientation. This approach based on free form surfaces shows conceptual limitations, if ramifications of rivers or floodplains are considered, as, in general, the domain cannot be described by a surface with 4 boundary curves. Nevertheless, b-spline surfaces allow suitable resolutions of high gradients in numerical computations of flow fields, if a user specific resolution is constituted. Consequently, b-spline surfaces are used to represent structures of the domain with dominant relevance for the flow field. In the presented case studies, structures such as river banks, levees and the river bed are approximated by b-spline surfaces.

Triangular irregular element meshes are highly adaptive to the fluvial topography. Without involving the smoothing property of b-spline surfaces triangular irregular element meshes enhance the accuracy of domain representation, whereas they are exposed to blunders in the original data set. Consequently, within the hybrid meshing scheme irregular triangle meshes are used for discretisations of the floodplains regions with inferior relevance for the flow field.

Generally, irregular triangle meshes are more suitable than b-spline surfaces to represent arbitrary shapes at a given accuracy level. The applicability of b-splines is enhanced within this hybrid scheme using the suggested breakline detection approach, which provides enhanced representations of the boundaries for these b-splines. Both, regular element meshes based on b-spline surfaces and triangular irregular element meshes are in use since decades for manual mesh generation using GIS systems. The hybrid meshing scheme joins available techniques for automated mesh generation for complex fluvial domains and enhances the representation for hydrodynamic computations based on feature detection. Its contribution facilitates the preparation of suitable meshes for hydrodynamic simulation based on vast remote sensing data sets, such as those from airborne LiDAR.

### 3.2 Enhancements of the Hybrid Meshing Scheme

In earlier publications [BerkhahnEtAl-2002] the regular element meshes were generated by creating the boundary curves of the b-spline surfaces manually. This means, the user had to select manually all control points defining these boundaries. The only support provided by the HydroMesh meshing tool were coloured displays of the topography. Where the colour indicates the height of all measurement points. This is a very time consuming task to select all control points, what is not acceptable for the user.

The hybrid meshing scheme in the version presented the first time by the authors [RathEtAl-2005] involves an automatic breakline detection. These breaklines were used to define the boundary curves of the b-spline surfaces, what leads to a dramatic reduction of user interactions and, consequently, a speed up of the whole meshing process. At this stage of development the breakline detection and slope classification were performed on linear interpolation analysis grids. These linear analysis grids lead to breaklines with a significant zigzag property. Therefore, the analysis grids were

enhanced by a b-spline based smoothing technique. In addition, a simple interpolation scheme is implemented in order to calculate slope values between analysis grid points. Both enhancements are explained in the following section.

## 4 Breakline Detection

The individual consideration of different sub domains of the topography is based on terrain feature recognition and especially on breakline identification. This terrain feature analysis and slope classification are performed on regular high resolution rectangular grids approximating the topography. Different slope determination methods are investigated by Rath and Pasche [RathPasche-2004] and are implemented within the analysis tool HybridMesh. The slope calculation for this study case is performed according to the one-over-distance method [Jones-1998]. The slope  $S_{ij}$  of a grid point  $\mathbf{d}_{ij}$  is given by:

$$S_{ij} = \arctan \left( \sqrt{S_{ij\ u}^2 + S_{ij\ v}^2} \right) 180/\pi \quad \text{with} \quad (1)$$

$$S_{ij\ u} = \frac{(z_{i+1j+1} + \sqrt{2}z_{i+1j} + z_{i+1j-1}) - (z_{i-1j+1} + \sqrt{2}z_{i-1j} + z_{i-1j-1})}{(4 + 2\sqrt{2}) |\Delta\mathbf{d}|}$$

$$S_{ij\ v} = \frac{(z_{i-1j+1} + \sqrt{2}z_{ij+1} + z_{i+1j+1}) - (z_{i-1j-1} + \sqrt{2}z_{ij-1} + z_{i+1j-1})}{(4 + 2\sqrt{2}) |\Delta\mathbf{d}|}$$

The term  $z_{ij}$  denotes the  $z$ -coordinate of all points of the analysis grid. The term  $|\Delta\mathbf{d}|$  represents the grid edge length in the  $xy$ -plane. The application of a linear slope analysis grid is presented by the authors in earlier publications [RathPasche-2004] [RathEtAl-2005]. Fig. 3 shows a detail of the topography with measurement points and a linear rectangular slope analysis grid. Grid points exceeding the limit slope value  $S_{lim}$  of 5 degrees are indicated by red dots. Characteristic for this approach is the zigzag course of breaklines, which is handled difficultly in the presented hybrid meshing scheme.

The first key idea of the breakline identification approach presented in this contribution is the use of b-spline technology in order to generate a rectangular analysis grid. The  $(N + 1) \times (M + 1)$  grid points  $\mathbf{d}_{ij}$  are equidistant in the  $xy$ -plane:

$$\Delta\mathbf{d} = \mathbf{d}_{i+1j} - \mathbf{d}_{ij} = \mathbf{d}_{i+1j+1} - \mathbf{d}_{ij} \quad (2)$$

for  $0 \leq i \leq N - 1, 0 \leq j \leq M - 1$

The distance  $|\Delta\mathbf{d}|$  is depending on the resolution of measurement points, the dimensions of the area under consideration and finally on the computer performance.

B-spline surfaces imply beneficial properties such as local modeling or smoothing. For the generation of b-spline analysis grids, the grid points  $\mathbf{d}_{ij}$  of the bilinear grid are interpreted as control points of a b-spline surface. The  $z$ -coordinates of the control points are determined by a dragging algorithm [BerkhahnEtAl-2002] which uses the  $z$ -coordinates of the bilinear grid points as starting values of the iteration process. The b-spline grid points  $\mathbf{b}_{ij}$  are defined in constant parameter distances  $\Delta u$  and  $\Delta v$  according to (4):

$$\mathbf{b}_{ij} = \mathbf{b}(u_K + (i - 1)\Delta u, v_L + (j - 1)\Delta v) \quad (3)$$

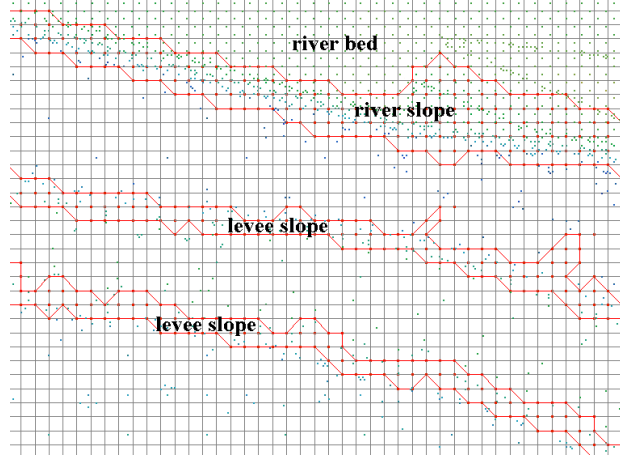


**Fig. 3.** Breakline identification based on a linear analysis grid (detail of case study 2: River Danube)

In order to ensure a moderate smoothing quadratic b-spline surfaces are chosen as analysis grid. In dependence of a parameter set  $u, v$  a point on the b-spline surface  $\mathbf{b}(u, v)$  is defined by double sum of all control points  $\mathbf{d}_{ij}$  multiplied by the corresponding b-spline functions  $N_i^K(u)$  and  $N_j^L(v)$ :

$$\mathbf{b}(u, v) = \sum_{i=0}^N \sum_{j=0}^M \mathbf{d}_{ij} N_i^K(u) N_j^L(v) \quad (4)$$

for  $u \in [u_K, u_{N+1}]$ ;  $v \in [v_L, v_{M+1}]$

In this formula the control points  $\mathbf{d}_{ij}$  represent a regular grid of  $(N+1) \times (M+1)$  points. The upper indices  $K$  and  $L$  indicate the degree of the b-spline functions. In order to ensure the property of local modeling the b-spline functions of degree 0 are defined as follows:

$$N_i^0(u) = \begin{cases} 1 & \text{for } u \in [u_i, u_{i+1}[ \\ 0 & \text{else} \end{cases} \quad \text{for } i = 0, \dots, N + K \quad (5)$$

In (5)  $u_i$  and  $u_{i+1}$  denote the lower and upper bounds of the  $i^{\text{th}}$  parameter interval. All bounds of the parameter intervals are gathered in a knot vector  $\mathbf{u}$ :

$$\mathbf{u} = [u_0, \dots, u_{N+K+1}]^T \quad (6)$$

The b-spline functions of degree  $r$  are given by the recursive formula:

$$N_i^r(u) = \frac{u - u_i}{u_{i+r} - u_i} N_i^{r-1}(u) + \frac{u_{i+r+1} - u}{u_{i+r+1} - u_{i+1}} N_{i+1}^{r-1}(u) \quad (7)$$

for  $r = 1, \dots, N + K$ ;  $i = 0, \dots, N + K + 1$

The second key idea is to eliminate the zigzag course of breaklines by an interpolation scheme for breakline points. Since the corresponding slope value is determined

for every grid point, it is obvious to interpolate the points with the exact limit slope value.

A cell of the analysis grid is given by four grid points  $\mathbf{b}_{ij}$ ,  $\mathbf{b}_{i-1j}$ ,  $\mathbf{b}_{ij-1}$  and  $\mathbf{b}_{i-1j-1}$ . On the edge  $\mathbf{b}_{ij}\mathbf{b}_{i-1j}$  a point  $\mathbf{p}_{\text{edge}1}$  is linearly interpolated by:

$$\mathbf{p}_{\text{edge}1} = \frac{S_{i-1j} - S_{\text{lim}}}{S_{i-1j} - S_{ij}} \mathbf{b}_{ij} + \frac{S_{\text{lim}} - S_{ij}}{S_{i-1j} - S_{ij}} \mathbf{b}_{i-1j} \tag{8}$$

for  $\text{sign}(S_{i-1j} - S_{\text{lim}}) \neq (S_{ij} - S_{\text{lim}})$

In general, this interpolation procedure for all four edges of a cell leads to two or four interpolation points  $\mathbf{p}_{\text{edge}}$ . The breakline point is determined by the mean value of these interpolation points. Fig. 4 shows the b-spline analysis grid, the slope points and the interpolated breakline points. These breaklines provide valuable terrain information for the river slope as well as for the floodplain. The identified terrain features are fundamental for the hybrid meshing scheme explained in the following sections.

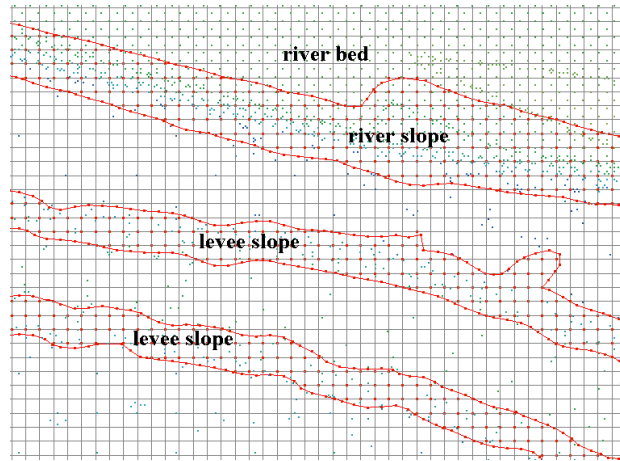


**Fig. 4.** Breakline identification based on a b-spline grid and breakpoint interpolation (detail of case study 2: River Danube)

## 5 Regular Meshes Based on B-Spline Surfaces

The topography is approximated by quadratic b-spline surfaces in order to facilitate the generation of a regular mesh with a specified edge ratio and element orientation.

### 5.1 B-Spline Surfaces Matching Breaklines

The identified breaklines are used for the efficient determination of control point grids defining the approximating b-spline surfaces. The user has to specify roughly

some boundary points of the control point grid and the control points are generated in the specified distance and are automatically moved to the nearest breakline. Fig. 5 illustrates a detail of the definition process, where the dark blue points indicate the boundary control points of b-spline surface. The interior control points are generated via a Coons interpolation scheme [BerkhahnEtAl-2002]. Points of the regular element mesh are determined by specified parameter distances  $\Delta u$  and  $\Delta v$  and by applying (4). Figure 6 shows the regular triangle mesh approximating the river bed and matching the identified breaklines.

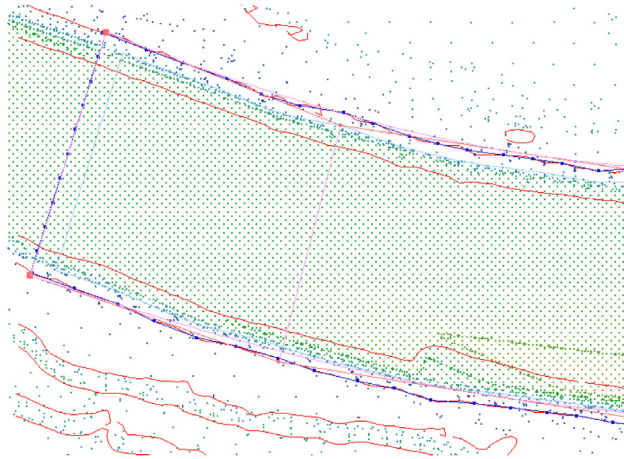


**Fig. 5.** Editor process with automatic identified breaklines (case study 2: River Danube)

## 5.2 Handling of Overlapping B-Spline Surfaces

A non ramified river bed could easily be approximated by b-spline surfaces: two opposed boundary curves of the surface approximate the shore lines of the river and the remaining two boundary curves represent the inflow and outflow cross section of the river section under consideration. This easy handling becomes more sophisticated while dealing with islands or tributaries. Berkhahn et al. [BerkhahnEtAl-2002] developed an approach to generate consistent element meshes for these cases. The key idea is to connect the different b-spline surfaces for the main stream and the tributaries consistently. This approach requires the usage of endpoint interpolating b-spline surfaces with multiple knots in the knot vectors. This manipulation of the knot vectors involves the serious disadvantage of a non uniform parameterisation of the b-spline surface and consequently the usage of constant  $\Delta u$  and  $\Delta v$  parameter distances for the generation of element nodes is impractical.

To cope with these circumstances, an approach with overlapping b-spline surfaces is developed. This approach is illustrated in figs. 7 and 8 for a small river detail of the first case study. Main river and tributary are approximated by two disconnected and overlapping b-spline surfaces. The corresponding control point grids

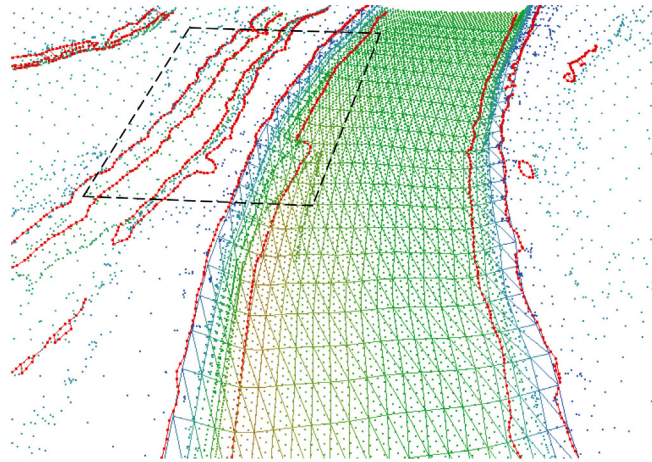


**Fig. 6.** Regular element mesh of the river bed matching identified breaklines (case study 2: River Danube); the dashed square indicates the detail of figs. 3 and 4

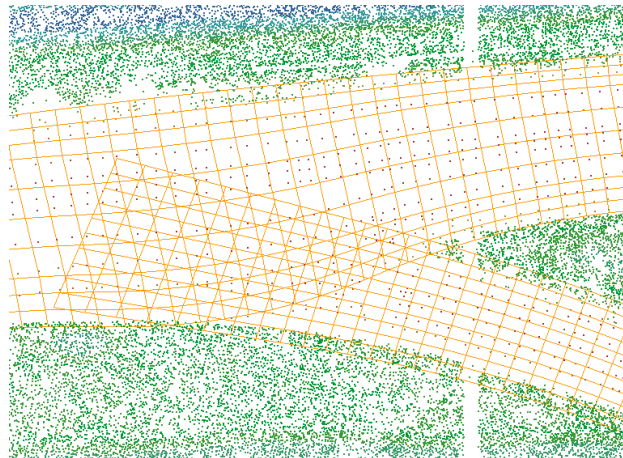


**Fig. 7.** Control point grids of two overlapping b-spline surfaces representing the main river and the tributary (case study 1: River Stoer)

are shown in fig. 7. In order to approximate the bank slope of the main river with higher accuracy the control points are concentrated in this area. Because both b-spline surfaces represent the same measurement points in the overlapping area the  $C^0$  and  $C^1$  continuity between these surfaces is ensured. Based on both surfaces, regular meshes are generated considering the specific meshing requirements. In a post process both meshes are stitched as illustrated in fig. 8. This approach of overlapping b-spline surfaces requires no difficult and sophisticated editor functionality to generate consistent control point grids and finally, this approach is easy to handle for the user.

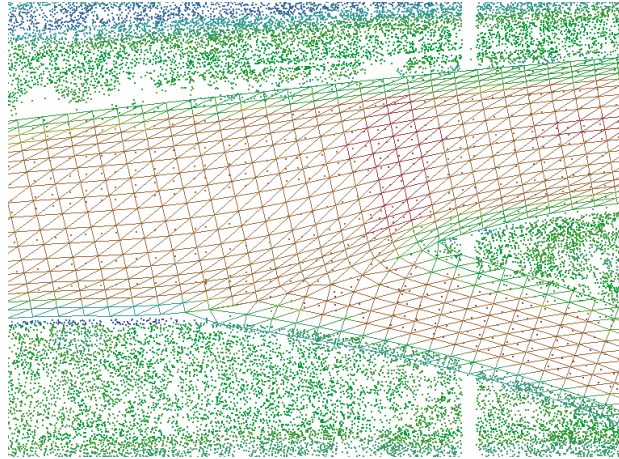


**Fig. 8.** Stitched element mesh of the main river and the tributary (case study 1: River Stoer)

### 5.3 Handling of Regular Grids with Arbitrary Boundaries

The b-spline meshing technique involves serious problems in the case of any arbitrary boundary of the considered domain. Due to the regular control point grid a b-spline surface is bounded by four boundary curves. If it is impossible to approximate the domain by a quadrilateral b-spline surface the face technology is applied. This face technology is well known in design of construction parts in free form modeling: The relevant area of a free form surface is cut out of the entire free form surface.

The same approach is used in the hybrid meshing scheme: For instance, the slope of a levee is approximated by a b-spline surface with a significant overhang. The face curve is based on the identified breaklines of the levee and represents a closed loop. All regular elements generated on the b-spline surface are deleted if at least one node of the element is located outside of the closed loop of the face curve. This approach involves the advantage to specify the edge ratio and orientation of the elements while the needless elements are neglected.

## 6 Irregular Triangle Meshes Adapted from Delaunay Triangulations

The hybrid meshing scheme involves irregular triangles for the floodplain. A Delaunay triangulation of point measurements efficiently provides irregular triangle meshes but involves a significant disadvantage: a one-to-one mapping of measurement points to mesh nodes is not suitable for the considered case studies, as they commonly deal with millions of points. Ruppert [Ruppert-1995] and Shewchuck [Shewchuck-2002] presented very effective refinement and coarsening schemes. In this contribution a more simple refinement and coarsening approach for the hybrid meshing scheme is used.

Aiming to generate a more or less uniformly dense, but irregular mesh on the floodplain, an initial Delaunay triangulation is performed for the original point set including all measurement points, all identified breakline points and all boundary nodes of regular partial element meshes. All points on the convex hull of the point set, on identified breaklines and on boundaries of regular partial meshes are fixed, i.e. no points are allowed to be moved or deleted.

A coarsening procedure collapses the points of a triangle or of a single edge by the corresponding center point if the edge length is below a user defined minimal edge length. The left hand side of fig. 9 shows the Delaunay triangulation of a point set (black points). This triangulation leads to two triangles each with 3 edges (red edges) below a specified minimum edge length. The corresponding points of the affected triangles are deleted and replaced by the center points (green points). The re-triangulation leads to a coarser mesh, but one single edge is still below the minimal edge length. As shown on the right hand side of fig. 9 the points corresponding to this edge (red edge) are deleted and replaced by their center point (green point). The re-triangulation leads to a coarse mesh with no edge below the minimal edge length.

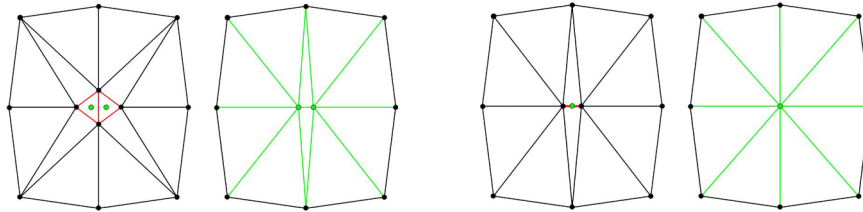


**Fig. 9.** Coarsening of triangles (left) and of a single edge (right)

A refinement procedure adds the corresponding center point if the edge length of a triangle or a single edge exceeds a user defined maximum edge length. The left hand side of fig. 10 shows the Delaunay triangulation of a point set (black points). This triangulation leads to two triangles each with 3 edges (red edges) exceeding a specified maximum edge length. The center points (green points) of these two affected triangles are added to the initial point set. The re-triangulation of this augmented point set leads to new edges (green edges) and to a refined triangle mesh. The right hand side of fig. 10 shows the Delaunay triangulation of a point set, where a single edge (red edge) exceeds the maximum edge length. The center point (green point) is added to the initial point set. The re-triangulation of this new point set leads to a refined triangle mesh with new edges (green edges) not exceeding the maximum edge length.

Finally, a Laplace smoothing is performed for all points not regarded to be fix. Fig. 11 shows the result of the refinement and coarsening procedure and the fixed breaklines. The triangulation and adaptations procedure concatenates regular and irregular element meshes as shown in figure 12.

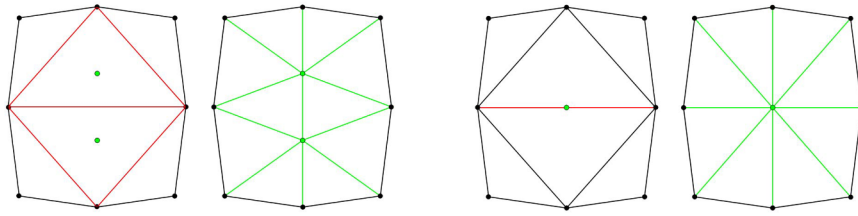


**Fig. 10.** Refinement of triangles (left) and of a single edge (right)

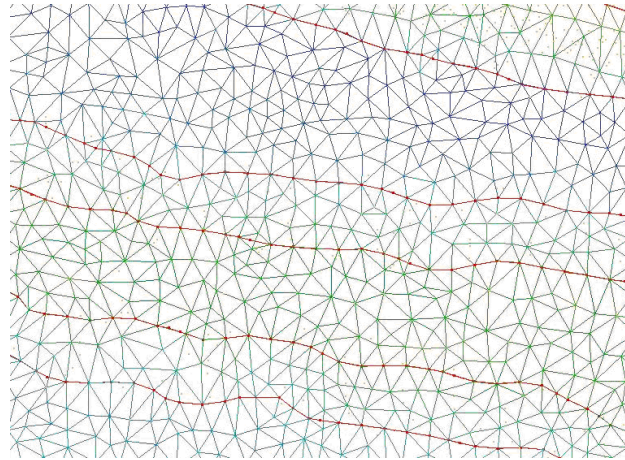


**Fig. 11.** Irregular triangle mesh matching identified breaklines (case study 2: River Danube)

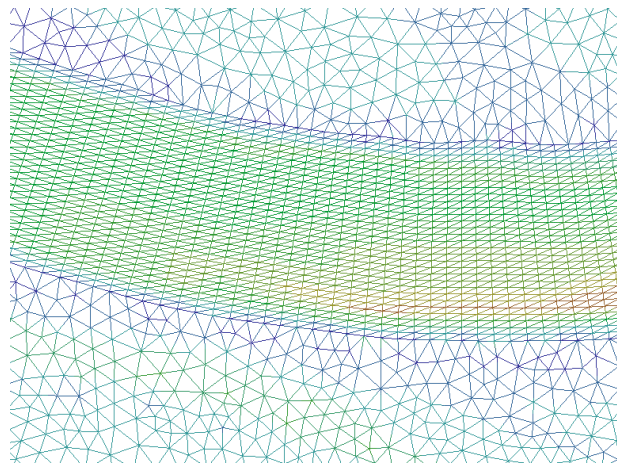


**Fig. 12.** Detail of the generated hybrid element mesh (case study 2: River Danube)

## 7 Quality Analysis for Hybrid Mesh Terrain Representation

For the case study 1 of the River Stoer the original Delaunay refinement [Ruppert-1995] [Shewchuck-2002] is applied to generate the triangle elements. The objective of this case study is the optimization of the final mesh with regard to the minimum element angle ( $\alpha \geq 20$  degrees) and the maximum element area size ( $A \leq 22 \text{ m}^2$ ). The entire mesh consists of 11,060 elements and 6,308 nodes. This extremely dense refinement is intended to obtain a mesh, which accurately resolves the flow gradients in the river junction.

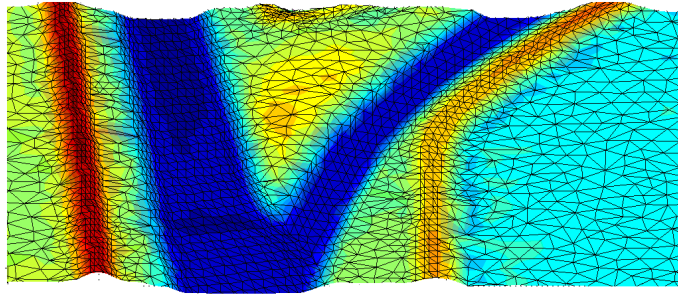


**Fig. 13.** Detail of the generated hybrid element mesh (case study 1: River Stoer)

The accuracy of the presented hybrid mesh is sampled for various ratios of the available measurements. A twofold classification criterion is applied, stating acceptable representations (green residuals), sufficient representations (yellow residuals) and those with significant deviation from the measured data (red residuals). With respect to the accuracy demands on LiDAR data for floodplain mapping [RathBajat-2004], the following classification for residuals is introduced.

**Table 1.** Classification for residuals

acceptable:	residuals $\leq \pm 0.10 \text{ m}$
tolerable:	$\pm 0.10 \text{ m} < \text{residuals} \leq \pm 0.30 \text{ m}$
significant:	$\pm 0.30 \text{ m} < \text{residuals}$

For a random sampling series 1%, 5%, 10% and 30% of the available measurements are considered. Anticipating one conclusion of this investigation, the sampling rate of 1% is sufficient to classify the mesh representation. The margin for classifications sampling more than 1% of measurements denotes less than 1.5% for each class. Further statistical measures such as the mean residual  $\mu_R$  and the standard deviation  $\sigma_R$  of the mesh representation provide essential information about the quality of the hybrid mesh. For the case study of the River Stoer, again 1% of samples provides a suitable impression of the statistical parameters. Additional sampling reveals a margin in standard deviation below 1 cm.

**Table 2.** Impact of random sampling ratios on quality assessment

Sampling Ratio	Green Residuals	Yellow Residuals	Red Residuals	Mean Residual $\mu_R$	Standard Deviation $\sigma_R$
1%	67.6%	29.5%	2.9%	0.023 m	0.153 m
5%	69.2%	27.3%	3.5%	0.021 m	0.146 m
10%	69.2%	27.2%	3.6%	0.022 m	0.154 m
30%	68.5%	27.8%	3.7%	0.022 m	0.158 m

Accuracy standards for floodplain mapping based on LiDAR data, given by the US Federal Emergency Management Agency in accordance with the US National Standard for Spatial Data Accuracy for digital products, claim that an accurate DEM should have a maximum Root Mean Square Error of 15 cm [FEMA-2003]. Moreover, 95% of any sufficiently large sample should be less than  $1.9600 \times \text{RMSE}$ , holding for normally distributed differences averaging zero. A RMSE of 15 cm denotes a "30 cm accuracy at the 95% confidence level" [FEMA-2004b].

For the validation of the mesh against these requirements, the mesh is considered as ground truth estimate and the measured data is considered as corresponding ground truth. Based on table 2 the terrain representation in fig. 13 is considered suitable for floodplain mapping. With  $\sigma_R \approx \text{RMSE} \approx 0.15$  m and since the magnitude of red residuals clearly ranges below 5% it is obvious, that the "30 cm accuracy at the 95% confidence level" is assured. For this case study, red residuals are partly raised by a drainage ditch, which is included in the LiDAR data set without being excluded in the hybrid mesh at the border between the b-spline mesh and its adjacent irregular triangle mesh. The relevance for a hydrodynamic simulation is negligible, though.

## 8 Numerical Simulation

This numerical simulation for the case study 1 shows a typical discharge scenario. Parts of the slightly elevated hook at the river junction appear as an island, surrounded by the flow of River Bramau and Stoer.

Generally, the representations of the slow velocity gradients are accurate, denoting the distinct shallow terrain. The visualisation of the water depths indicates the sensitivity of hydrodynamics with regard to the mesh topology. The drainage ditch represented in fig. 14 is represented despite a local lack of data (see fig. 1). The water depths indicate a local pit. Consequently, the velocity field in figs. 14 and 15 is dominated by turbulent structures that are likely to be representative for that spot. For coarser meshes such representations might generally lead to troublesome numerical stability demands.

## 9 Conclusion

This contribution presents an efficient technique to generate adaptable element meshes for an accurate representation of terrain data in numerical simulations. In-

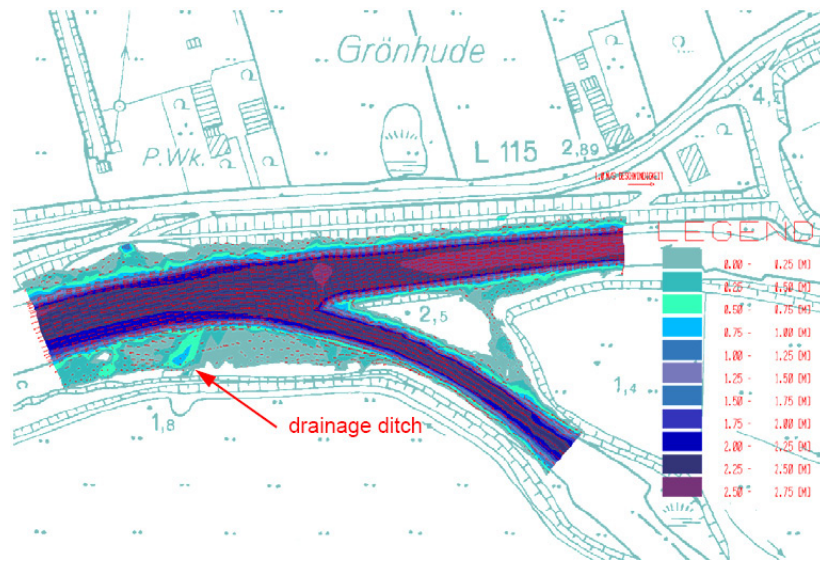


Fig. 14. Water depths and velocity vectors for typical discharge scenario of the River Stoer and Bramau (case study 1)

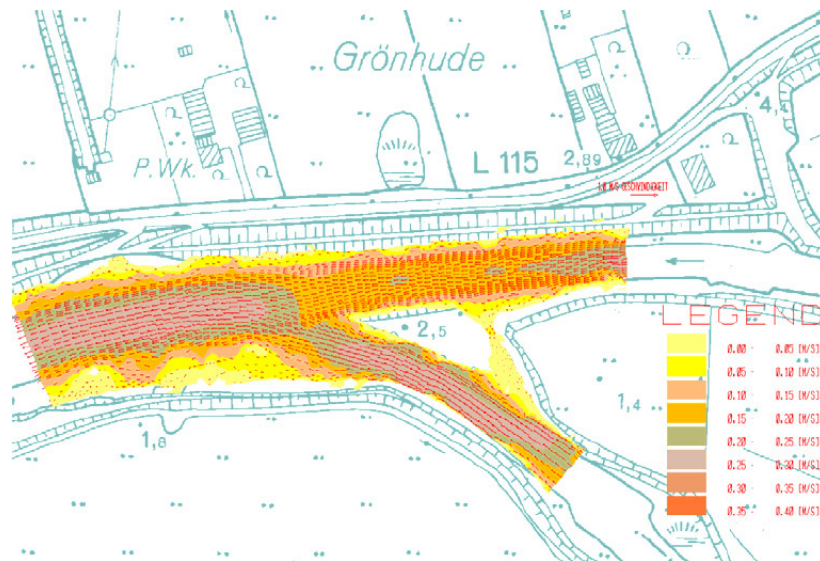


Fig. 15. Velocity field with flow vectors for a typical discharge scenario of the River Stoer and Bramau (case study 1)

terpolated breakline points determined on rectangular b-spline analysis grids are suitable to provide the essential terrain features in shallow fluvial domains with sufficient accuracy. Breakline identification is fundamental for the hybrid meshing scheme introduced by the authors. Regular element meshes use these breaklines to define the boundary for b-spline surfaces approximations for river beds, banks, groynes and any other flow relevant sloped terrain feature. In floodplain areas, represented with irregular triangle meshes, these breaklines are matched by element edges in order to represent terrain features accurately. Case studies demonstrate the usability and suitability of the presented hybrid meshing scheme based on breakline identification for hydrodynamic simulations.

## 10 Acknowledgements

The author Kai Kaapke wishes to acknowledge the support of the German Academic Exchange Service (DAAD) within the postgraduate research program during his year-long stay at the Water Research Laboratory in Australia.

- [BerkhahnMai-2004a] Berkhahn V, Mai S (2004) Meshing bathymetries for numerical wave modeling. Proceedings of the 6th International conference on Hydroinformatics 2004. World Scientific Publishing Co. Pte. Ltd., Singapore, Vol. 1: 47-54
- [BerkhahnMai-2004b] Berkhahn V, Mai S (2004) Numerical Wave Modeling based on Curvilinear Element Meshes. Proceedings of the 4th International Symposium on Environmental Hydraulics, ISEH04, Hong Kong
- [BerkhahnEtAl-2002] Berkhahn V, Göbel M, Stoschek O, Matheja A (2002) Generation of Adaptive Finite Element Meshes Based on Approximation Surfaces. Proceedings of the 5th International Conference on Hydro-Science and -Engineering, ICHE 2002, Warsaw, Poland
- [FEMA-2004a] FEMA, Federal Flood Emergency Management Agency (2004) Flood Hazard Mapping - Hydraulic Models Meeting the Minimum Requirement of NFIP. National Accepted Models.  
<http://www.fema.gov/fhm/enhydra.shtm> (14.02.2005)
- [FEMA-2004b] FEMA, Federal Flood Emergency Management Agency (2004) Quality Control / Quality Assurance for Flood Hazard Mapping.  
<http://www.fema.gov/fhm/dlqgs.shtm> (14.02.2005)
- [FEMA-2003] FEMA, Federal Flood Emergency Management Agency (2003) Guidelines and Specifications for Flood Hazard Mapping Partners.  
<http://www.fema.gov/mit/tsd/mma4b7.shtm> (14.02.2005)
- [Goebel-2005] Göbel M (2005) HydroMesh Meshing Tool. [www.hydromesh.com](http://www.hydromesh.com) (31.3.2005)
- [Jones-1998] Jones K H (1998) A comparison of algorithms used to compute hill slope as a property of the DEM. Computers & Geoscience, Vol. 24: 315-323
- [RathEtAl-2005] Rath S, Pasche E, Berkhahn V (2005) Modeling High Resolution Remote Sensing Data for Flood Hazard Assessment. Proceedings of ASPRS 2005, American Society for Photogrammetry & Remote Sensing, Baltimore, Maryland

- [RathPasche-2004] Rath S, Pasche E (2004) Hydrodynamic Floodplain Modeling based on High-Resolution LiDAR measurements. Proceedings of 6th International Conference on Hydroinformatics 2004. World Scientific Publishing Co. Pte. Ltd., Singapore, Vol. 1: 486-493
- [RathBajat-2004] Rath S, Bajat B (2004) Between Sensing, Forecasting and Risk Assessment: An Integrated Method to Model High Resolution Data for Floodplain Representations in Hydrodynamic Simulations. Proceedings of 1st Goettingen Remote Sensing Days 2004, Goettingen 07-08 October. In: Erasmi S, Cyffka B, Kappas M (eds) Remote Sensing & GIS for Environmental Studies. Goettinger Geographische Abhandlungen, Bd. 113, Verlag Erich Goltze, Goettingen, Germany
- [Ruppert-1995] Ruppert J (1995) A Delaunay refinement algorithm for quality 2D-mesh generation. Journal of Algorithms, Vol. 18, No.3: 548-585
- [Shewchuck-2002] Shewchuck J R (2002) Delaunay refinement algorithms for triangular mesh generation. Computational Geometry: Theory and Applications, Vol. 22 (1-3): 21-74

